Magnetic moments of the isomeric states of ^{141}Pr and ^{143}Pm and the paramagnetism of promethium and praseodymium

B. I. Gorbachev, A. I. Levon, O. F. Nemets, S. N. Fedotkin, and V. A. Stepanenko

Institute of Nuclear Research, Academy of Sciences of the Ukrainian SSR, Kiev
(Submitted 21 October 1983)
Zh. Eksp. Teor. Fiz. **87**, 3–13 (July 1984)

The g-factors of the $11/2^-$ and $15/2^+$ isomeric states of the ^{141}Pr and ^{143}Pm nuclei (Tables I and II) have been measured by the method of differential and integrated perturbed angular distribution. The parametric corrections were determined for ^{143}Pm from the measured temperature dependence $g\beta(T)$. The relaxation times have been measured for nuclear states aligned in beam reactions, metal targets, and targets made of La and Pr oxides. The results are analyzed in terms of the quasiparticle-phonon model with allowance for the spin-multipole interaction.

Odd nuclei with neutron number $N = 82$ exhibit well-defined shell properties. Their low-lying states can be described in a relatively simple and small configuration space.[1–8] It has been shown that these states constitute mainly proton excitations and are satisfactorily described by the weak-coupling model,[5,6] the shell model,[1,7,8] and the Tamm-Dancoff approximation.[2,3] Magnetic moments are a good testing ground for wave functions of such states. However, it must then be remembered that the discrepancy between the measured magnetic moments and the single-particle values is influenced in an important way by a number of specific effects, the most important of which is the spin polarization of the core and meson exchange currents.[9]

To estimate the effects due to the spin polarization of the core, we must know the spin-spin interaction responsible for them and the energy difference between the sublevels with $j = l \pm 1/2$. These parameters can be obtained by comparing theoretical calculations based on the quasiparticle-phonon model with experimental data on the localization and strength of $M1$ excitations in even-even nuclei. Studies of the enhancement and blocking of core polarization can be used as experimental verifications of the level occupation numbers near the Fermi surface, since the polarization effect for magnetic moments depends on the configuration of the filled shells. The variation in the g-factors as one departs from a magic core may be due to the contribution of collective components of the motion, and these must be taken into account when core polarization effects are investigated.

We have measured the g-factor of $11/2^-$ and $15/2^+$ states of ^{141}Pr and ^{143}Pm and have analyzed them in the light of the above effects. The lifetimes of the isomeric states have been remeasured. Paramagnetic corrections that must be taken into account when the g-factor is deduced from experimental data depend on the charge state of rare-earth ions. The measurements were performed at different temperatures in order to determine the charge state of the ions and to verify the calculated paramagnetic corrections given in Ref. 10. We have also measured the nuclear-orientation relaxation times due to paramagnetic and quadrupole interactions. Preliminary results were published in Ref. 11.

METHOD AND RESULTS

The isomeric states were excited and aligned in ^{139}La$(\alpha,2n)^{141}$Pr and ^{141}Pr$(\alpha,2n)^{143}$Pm) reactions in a pulsed beam of 27-MeV α-particles produced by the U-120 cyclotron of the Institute for Nuclear Studies of the Ukrainian Academy of Sciences. The decay scheme for the isomeric states is shown in Fig. 1. The method of differential perturbed angular distribution of γ-rays was used to measure the g-factors of the $11/2^-$ and $15/2^+$ states of ^{143}Pm and the $11/2^-$ state of ^{141}Pr. The method is described in detail in Ref. 12. The high-frequency accelerating voltage of the cyclotron was used to define the time scale. The target was located in a magnetic field B whose direction was perpendicular to the plane of the reaction. If the unperturbed angular distribution of the γ-rays can be written in the form

$$W(\theta) = \sum_k b_k \cos k\theta,$$

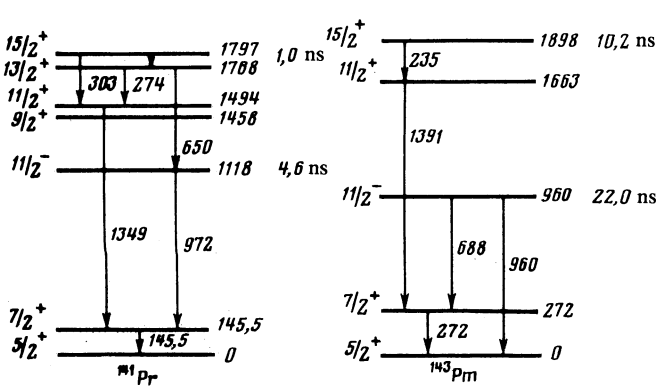

FIG. 1. Decay scheme for the isomeric states of ^{141}Pr and ^{143}Pm.

 0038-5646/84/070001-06$04.00 © 1985 American Institute of Physics

the intensity of γ-rays emitted as a result of the decay of the isomeric state in the magnetic field has the form

$$N(\theta, B, t) = N_0 \exp\left(-\frac{t}{\tau}\right) \sum_k b_k G_k(t) \cos k(\theta - \omega_L t).$$

where N_0 is the intensity at time $t = 0$, τ is the lifetime of the isomer, ω_L is the Larmor precession frequency, and $G_k(t)$ is the perturbation factor due to interactions in the target. The g-factor data were deduced from the normalized difference between time spectra (1) at $\theta = \pm 135°$ to the incident beam (corrected for deflection in the magnetic field):

$$R(\theta, B, t) = \frac{N(+135°) - N(-135°)}{N(+135°) + N(-135°)} = -b_2 G_2(t) \sin 2\omega_L t \quad (2)$$

subject to the condition that $b_2 \gg b_4$.

These g-factor measurements on rare-earth nuclei were complicated by the paramagnetic interaction between $4f$-electrons and nuclei. Polarization of the $4f$-electrons in the external magnetic field produces a paramagnetic enhancement of the field at the nuclei, and the Larmor precession frequency becomes $\omega_L = g\mu_N \beta B/\hbar$. The paramagnetic correction β was calculated by Günther and Lindgren[10] to within 5% (their estimate). However, measurements of β for europium[13] and gadolinium[14] as a function of temperature show that the discrepancy as compared with the calculated β was much greater. In these experiments, extrapolation of $g\beta$ to infinite temperature yielded the g-factor and, consequently, β as a function of temperature. Low-lying atomic excited states influence the paramagnetic corrections for europium and gadolinium. There is very little information on the validity of such calculations for other elements for which the contribution due to the excited atomic states is negligible. Moreover, paramagnetic corrections depend on the charge state of the recoil ions in the crystal lattice of the target, which can also be determined from the function $\beta(T)$. This function was measured for praseodymium in Ref. 15, and the corresponding measurements on promethium are reported below.

The second factor that complicates such measurements is the rapid decay of the function $R(\theta, B, t)$ due to random fluctuations in the strong paramagnetic field and the electric-field gradient of the $4f$-shells. The static quadrupole interaction in the densely-packed hexagonal lattice of the La and Pr metal targets should not give rise to appreciable loss of nuclear orientation because the lattice spacing ratio c/a for these targets is 1.606 and 1.616, respectively, i.e., it is close to the value $2\sqrt{2/3}$ at which the static electric-field gradient is zero. This is confirmed by measurements[16] on the zirconium hexagonal lattice with a close c/a ratio. Nevertheless, it turns out that the reduction in the case of the metal target is greater than for an oxide target with a cubic lattice.[11] Measurements of $\beta(T)$ were therefore performed on a Pr_2O_3 target.

The target area and thickness were 4×5 mm and 40 mg/cm^2, respectively. The target was maintained in contact with a tantalum substrate with the aid of a 1.5-micron tantalum foil welded to the substrate over the perimeter of the target. The target was heated in one of two ways: by passing a current through the substrate or by placing the substrate in contact with a copper rod heated by a nichrome coil. A liquid-nitrogen cryostat placed in contact with the other end of the copper rod was used to cool the target. The target temperature was measured by a thermocouple welded to the substrate.

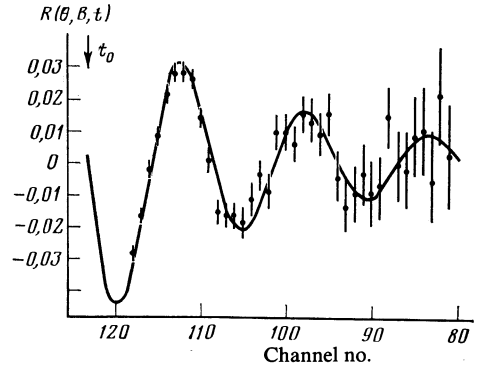

FIG. 2. Modulation of the intensity of the 1392-keV γ-rays from the ^{141}Pr $(\alpha, 2n)$ ^{143}Pm, reaction, due to the precession of ^{143}Pm during the decay of the $15/2^+$ isomer in the external field $B = 2.681(5)$ T at $T = 435$ K. Pr_2O_3 target: $\omega_L = 212(8)$ MHz; τ_R 22(7) ns.

The temperature dependence of the paramagnetic correcion $\beta(T)$ for ^{143}Pm in the Pr_2O_3 lattice was determined by measuring the Larmor precession frequency ω_L for the 1392-keV γ-transition at a number of temperatures in the range between 155 and 595 K in a constant external magnetic field of 2.681(5)T. [Here and henceforth, the notation 2.681(5) means 2.681 ± 0.005.] Figure 2 shows the modulation of the 1392-keV gamma-ray intensity measured by two NaI(Tl) detectors (length 50 mm, diameter 40 mm) for a target temperature of 435 K. The rapid decay of the function $R(\theta, B, t)$ corresponds to a relaxation time $\tau_R = 22(7)$ ns. Figure 3 shows the measured $g\beta$ as a function of temperature. According to Ref. 10, a departure from the $1/T$ dependence, i.e., from the function

$$\beta = 1 + g_J \mu_B (J+1) B_i(0)/3kT, \quad (3)$$

should occur above 500 K, where g_J is the electron g-factor, μ_B is the Bohr magneton, J is the angular momentum of the paramagnetic ion, k is Boltzmann's constant, and $B_i(0)$ is the hyperfine field experienced by the nucleus. The experimen-

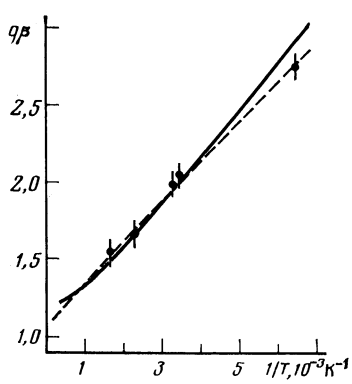

FIG. 3. Temperature dependence of $g\beta$ for the $15/2^+$ state of ^{143}Pm. Pr_2O_3 target. Solid curve—fit to the numerical data given in Ref. 10, broken line—fit to Eq. (4).

tal points in Fig. 3 were therefore fitted with numerical values of β taken from Ref. 10, multiplied by the g-factor which was treated as an adjustable parameter (solid line). The result was $g(\frac{15}{2}^+, {}^{143}\mathrm{Pm}) = +1.02(5)$. As can be seen from the figure, the discrepancy between the experimental points and the values calculated[10] for Pm^{3+} does not exceed the experimental uncertainty, except for the point at the temperature of 155 K.

According to published data,[17] the magnetic susceptibility of light rare-earth metals follows the Hund law ($\sim 1/T$). The deviation from the $1/T$ behavior, which has also been observed[15] for ^{143}Pr, may be considered to be due to the interaction between ions during implantation as a result of recoils. If this is so, the magnetic susceptibility and the paramagnetic correction should follow the Curie-Weiss law

$$\beta=1+g_J\mu_B(J+1)B_i(0)/3k(T-\Theta). \quad (4)$$

Figure 3 shows the fit achieved on the basis of this formula (dashed line). The result obtained for the paramagnetic Curie point is $\Theta = -15(7)$ K and the g-factor is $g = 1.05(5)$. The average obtained from these two fits is

$$g({}^{15}/_2{}^+, {}^{143}\mathrm{Pm})=1{,}03(5).$$

Figure 4 shows the modulation of the 688-keV γ-ray intensity from the ^{141}Pr(α,2n ^{143}Pm reaction. The measurements were performed on an oxide target at 435 K. The g-factor was calculated with the paramagnetic correction[10] $\beta = 1.63$. The result obtained for the $11/2^-$ state was $g(\frac{11}{2}^-, {}^{143}\mathrm{Pm}) = 1.23(7)$. This is somewhat higher than our experimental value[11] $g = 1.10(8)$ and the value $g = 1.14(9)$ published in Ref. 18. The temperature was not measured in Refs. 11 and 18 and was assumed to have room value. The relaxation time is the same, to within experimental error, as the value obtained for the $15/2^+$ state which has a similar g-factor.

Figure 5 shows the experimental results for the $11/2^-$ state of ^{141}Pr. The measurements were performed on a lanthanum metal target and on the oxide La_2O_3. The Larmor precession frequency is the same for both targets to within experimental error, i.e., the charge states of the recoil ions are the same. For the recoils in cerium, the charge state of praseodymium has been identified[5] as Pr^{3+}.

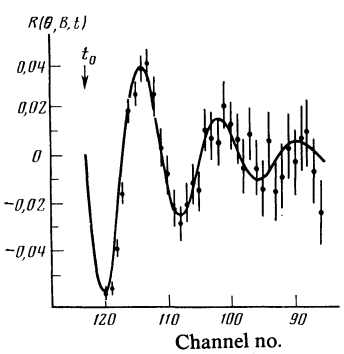

FIG. 4. Modulation of the intensity of the 688-keV γ-rays from the ^{141}Pr (α, 2n) ^{143}Pm reaction, due to the precession of ^{143}Pm during the decay of the $11/2^-$ isomer in the external field $B = 2.681(5)$ T at $T = 435$ K. Pr_2O_3 target: $\omega_L = 254(12)$ MHz; $\tau_R = 18(6)$ ns.

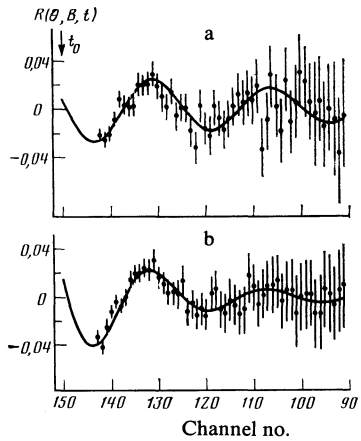

FIG. 5. Modulation of the γ-ray intensity from the ^{139}La (α, 2n) ^{141}Pr reaction, due to the precession of ^{141}Pr during the decay of the $11/2^-$ isomer in the external magnetic field $B = 2.905(12)$ T at $T = 330$ K: a—La_2O_3 target: $\omega_L = 298(20)$ MHz, $\tau_R = 27(9)$ ns; b—metal target: $\omega_L = 306(45)$ MHz, $\tau_R = 8.4(2.4)$ ns.

The paramagnetic correction $\beta = 1.91$, taken from Ref. 10, was used to calculate the g-factor. The average g-factor was found to be $g(\frac{11}{2}^-, {}^{141}\mathrm{Pr}) = 1.13(8)$. The g-factor for this state had previously been measured by the Japanese group[19] and their result was $g = 1.30(8)$. The 16% difference cannot be explained by systematic uncertainties. The quadrupole interaction was eliminated in Ref. 19 by heating the lanthanum metal target to 900 K. The external field was 1.90 T and the effective field at this temperature was 2.54 T, which contrasts with the value of 5.63 T in our case. This enabled us to observe only part of the precession period for the 4.6-ns isomer. The attenuation of the function $R(\theta, B, t)$ was not taken into account. These two circumstances may have been the origin of the systematic uncertainty in the measured Larmor precession frequency.

After subtracting the background, the sum of time spectra (1) can be used to determine the lifetimes of the isomeric states. The results are in agreement with previous measurements.[7,8] A summary of experimental data is given in Table I.

The g-factor of the $15/2^+$ state of ^{141}Pr was measured by the method of integrated perturbed angular distribution in an external magnetic field of 2.912 (12) T using two Ge(Li) detectors mounted at $\pm 135°$ to the beam incident on the target. For the γ-transition lying in a cascade with the isomeric transition, the angular distribution obtained for a target placed in a magnetic field pointing in the upward direction can be written in the form (when $A_2 \gg A_4$)

$$W(\theta)\uparrow = \mathrm{const}\left\{1+\frac{A_2G_2}{4+A_2G_2}\frac{I_d}{I_d+I_f}\left[1+\frac{3\cos 2(\theta-\Delta\theta_2-\Delta\theta_B)}{[1+(2G_2\omega_L\tau)]^{1/2}}\right] + \frac{A_2}{4+A_2G_2}\frac{I_f}{I_d+I_f}[1+3\cos 2(\theta-\Delta\theta_B)]\right\} \quad (5)$$

where A_2, A_4 are the coefficients in the angular distribution of γ-ray written in the form $\varepsilon A_h P_h \cos(\Theta)$, I_d is the intensity of the delayed component of the transition, I_f is the intensity of the fast component of the transition, and $\Delta\theta_B$ is the angle

TABLE I. Measurements of g-factors, lifetimes, and relaxation times by the method of differential perturbed angular distribution of γ-rays.

Nucleus, I^{π}	Target	$T_{1/2}$, ns	T, K	$g\beta$	g	τ_R, ns
^{143}Pm, $^{15}/_2{}^+$	Metal	10,5(6)	300	1,93(9)	1,01(5)	12(7)
		10,1(5)	593	1,54(6)	1,06(4)	32(10)
		10,1(5)	435	1,65(7)	1,01(4)	22(8)
	Oxide	10,2(5)	305	2,04(6)	1,06(3)	25(8)
		9,8(5)	305	1,98(6)	1,03(3)	20(7)
		10,5(5)	155	2,74(6)	0,96(3)	14(6)
		10,2(5) *			1,03(5) *	
^{143}Pm, $^{11}/_2{}^-$	Metal	22(1)	300	2,34(7)	1,22(4)	15(8)
	Oxide	21(1)	435	2,02(7)	1,23(4)	18(6)
		22(1) *			1,23(7) *	
^{141}Pr, $^{11}/_2{}^-$	Metal	4,6(1)	330	2,20(32)	1,15(15)	8,4(2,4)
	Oxide	4,7(2)	330	2,14(14)	1,12(8)	27(9)
		4,6(1) *			1,13(8) *	

*Average value

through which the beam rotates in the magnetic field. The rotation of the beam was compensated by turning the detectors through the angle $\Delta\theta_B$. The normalized difference between the photopeak areas after the subtraction of the background with the field up and down, respectively, is

$$R(\theta,B,t)=\frac{W(\theta+\Delta\theta_B)\uparrow+W(-\theta-\Delta\theta_B)\downarrow-W(-\theta+\Delta\theta_B)\uparrow-W(\theta-\Delta\theta_B)\downarrow}{W(\theta+\Delta\theta_B)\uparrow+W(-\theta-\Delta\theta_B)\downarrow+W(-\theta+\Delta\theta_B)\uparrow-W(\theta-\Delta\theta_B)\downarrow}$$

$$=\frac{I_d}{I_d+I_f}\frac{3A_2G_2}{4+A_2G_2}[1+(2G_2\omega_L\tau)^2]^{-1/2}\sin 2\theta\sin 2\Delta\theta_2. \qquad (6)$$

The angle $\Delta\theta_2$ is defined by $\mathrm{tg}\,2\Delta\theta_2=2G_2\omega_L\tau$, and the integrated attenuation factor is given by $G_2=\tau_R/(\tau+\tau_R)$.

The precession frequency was found as a result of a numerical solution of (6). We used the value of τ_R obtained by the method of differential perturbed angular distribution of γ-rays. The intensities of delayed and fast components were deduced from experimental data.[8] The coefficients of the angular distribution were determined from published data[8] and from independent measurements. The coefficient A_2 for the fast component of the γ-transition was determined from the formula

$$A_2^{\exp}=\frac{I_d}{I_d+I_f}G_2A_2+\frac{I_f}{I_d+I_f}A_2. \qquad (7)$$

Measurements were performed for two γ-ray transitions: namely, 1349 and 650 keV. The published[8] lifetime of the isomeric state is $\tau=1.44(14)$.

The paramagnetic correction $\beta=1.94(10)$ at the temperature of 320 K at which the measurements were performed was taken from Ref. 10. Table II lists the experimental results averaged over four independent exposures. The average result is: $g(\frac{15}{2}+{}^{141}\mathrm{Pr})=1.06(23)$.

DISCUSSION

According to the single-particle model, the additivity rule for magnetic moments, the g-factors of $(\pi 1h_{11/2})^n$-states in nuclei with $N=82$ should be equal. Figure 6 shows the experimental results for nuclei near ^{144}Gd with the magic number $Z=64$. One of the reasons for the departure from the additivity rule is the spin polarization of the core. Depending on whether the $1g_{7/2}$ or $2g_{5/2}$ level is filled with protons, one observes the enhancement or blocking of the $M1$-polarization of the core (curves 2 and 1). The corrections to the single-particle g-factors were calculated within the framework of the configuration mixing theory[20] (in the first order, using the harmonic-oscillator potential and interaction parameter $C=30$ MeV). They do not explain the deviations from the additivity rule. Moreover, if we use spectroscopic factors from stripping and pickup reactions[4] to calculate the occupation numbers, we obtain a diffuse distribution of the core protons over the $gdhs$ shell levels. The g-factors calculated for this case correspond to curve 3 in Fig. 6. The more rapid reduction in the g-factors with distance from ^{144}Gd may be due to the admixture of collective states.

The isomeric $11/2^-$ states of ^{141}Pr and ^{143}Pm can be described in terms of the quasiparticle-phonon model.[21,22] The Tamm-Doncoff method and the random-phase method[3,23–25] were used to explain the g-factors in this region. Core polarization is taken into account exactly in these models. The quasiparticle-phonon model takes core polarization into account by including the spin-multipole interaction in the analysis. In addition to core polarization, the model also takes into account 2^+- and 3^--collective excitations of the core. The model Hamiltonian is

$$H=H_0(n)+H_0(p)+H_M+H_{SM}, \qquad (8)$$

TABLE II. Measured g-factors of the $15/2^+$ state of ^{141}Pr.

E_γ, keV	$\frac{I_d}{I_d+I_f}$	$A_2^{\exp}$	A_2	G_2	R	g
1349	0,6(1)	0,27(5)	0,296	0,855(17)	−0,0493(25)	0,95(45)
650	0,79(3)	−0,17(2)	−0,192(32)	0,855(17)	0,0446(20)	1,10(26)
						1,06(23) *

* Average value

where $H_0(n)$ and $H_0(p)$ are the Hamiltonians describing the mean field and the neutron-proton pairing, whereas H_M and H_{SM} are the sums of the isoscalar and isovector separable multipole and spin-multipole interactions, respectively. They are given by

$$H_M = -\frac{1}{2}\sum_{\lambda}(\chi_0^{(\lambda)}+\chi_1^{(\lambda)}\tau_1\tau_2)\sum_{\mu}M_{\lambda\mu}^{+}M_{\lambda\mu}, \tag{8a}$$

$$M_{\lambda\mu}^{+} = \sum_{jj'}\sum_{mm'}\langle jm|i^{\lambda}r^{\lambda}\mathbf{Y}_{\lambda\mu}(\Omega)|j'm'\rangle a_{jm}^{+}a_{j'm'}, \tag{8b}$$

$$H_{SM} = -\frac{1}{2}\sum_{\lambda}\sum_{h=\lambda,\lambda+1}(\chi_0^{(\lambda L)}+\chi_1^{(\lambda L)}\tau_1\tau_2)\sum_{M}(S_{LM}^{\lambda})^{+}S_{LM}^{\lambda}, \tag{8c}$$

$$(S_{LM}^{\lambda})^{+} = \sum_{jj'}\sum_{mm'}\langle jm|i^{\lambda}r^{\lambda}[\sigma\mathbf{Y}_{\lambda\mu}(\Omega)]_{LM}|j'm'\rangle a_{jm}^{+}a_{j'm'}, \tag{8d}$$

$$[\sigma\mathbf{Y}_{\lambda\mu}(\Omega)]_{LM} \equiv \sum_{\nu\mu}\langle 1\nu\lambda\mu|LM\rangle\sigma_{\nu}\mathbf{Y}_{LM}(\Omega), \tag{8e}$$

where $\chi_0^{(\lambda)}$ and $\chi_1^{(\lambda)}$ are the isoscalar and isovector multipole interaction constants, $\chi_0^{(\lambda L)}$ and $\chi_1^{(\lambda L)}$ are the isoscalar and isovector spin-multipole interaction constants, $M_{\lambda\mu}$ is the multipole moment operator, S_{LM}^{λ} is the spin-multipole operator, S_{LM}^{λ} is the spin-multipole operator, a_{jm}^{+}, a_{jm} are the creation and annihilation operators, and σ is the spin operator.

We have confined our attention to the quadrupole and octupole and also spin-monopole interactions, i.e., we took $\lambda = 2$ and 3 in (8a, b) and $\lambda = 0$, $L = 1$ in (8c–e). The constants $\chi^{(2)}$ and $\chi^{(3)}$ were chosen so as to ensure the correct level energies for the lowest-lying 2^+- and 3^--states of the corresponding even-even nuclei, and the constants $\chi^{(01)}$ were deduced from the position of the M 1-resonance.[26] The following expressions were employed:

$$\chi_1^{(01)} = -4\pi\cdot 28/A, \quad \chi_0^{(01)} \approx 0{,}8\chi_1^{(01)} \tag{9}$$

If we now transform to the quasiparticle α_{jm}^{+}, α_{jm} and phonon $Q_{\lambda\mu i}^{+}$ operators (details can be found in Refs. 21 and 22), the wave function for an odd spherical nucleus corresponding to the Hamiltonian (8) with $\lambda = 2$ and 3 for the multipole interaction and $\lambda = 0$, $L = 1$ for the spin-multipole interaction, assumes the form

$$\psi(IM) = C_I\Big\{\alpha_{IM}^{+} + \sum_{\substack{\lambda=2,3,\\ i,j}} D_j^{\lambda i}(I)\,[\alpha_{im}^{+}\tilde{Q}_{\lambda\mu i}^{+}]_{IM}^{+} \times \sum_{ij} D_j^{1i}(I)\,[\alpha_{jm}^{+}\tilde{Q}_{1\mu i}]_{IM}\Big\}\psi_0, \tag{10}$$

where

$$[\alpha_{jm}^{+}\tilde{Q}_{\lambda\mu i}^{+}]_{IM} = \sum_{m}\langle jm\lambda\mu|IM\rangle\alpha_{jm}^{+}\tilde{Q}_{\lambda\mu i}^{+},$$

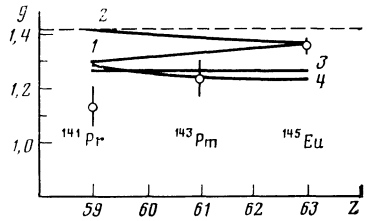

FIG. 6. Measured and calculated g-factors of the $11/2^-$-states of ^{141}Pr, ^{143}Pm, and ^{145}Eu: blocking (curve 1) and enhancement (curve 2) of proton polarization in the core, core polarization with the measured occupation numbers (curve 3), and calculations within the framework of the quasiparticle-phonon model (curve 4). Broken line—single-particle g-factor.

and the expressions for the coefficients C_I and $D_j^{\lambda i}$ can be found in Refs. 21 and 22.

For the g-factor of a state described by the wave function (10), we may write

$$g_I = C_I^2(g_{sp}+g_1^{(2)}+g_1^{(3)}+g_2), \tag{11}$$

where g_1 is the diagonal part of the matrix element g_I over the quadrupole and octupole phonons of the wave function (10) (off-diagonal elements are negligible), g_2 is the part of the matrix element g_I that is linear in the coefficients D_j^1, which is due to the M 1-phonons and represents the core polarization effect [the quadratic part in $(D_j^1)^2$ is small], and g_{sp} is the single-particle g-factor. Numerical calculations of the components of the wave functions were carried out in accordance with Refs. 27 and 28.

Table III lists the values of the coefficients C_I^2, the quantities g_{sp}, the quadrupole and octupole phonon contributions $g_1^{(2)}$ and $g_1^{(3)}$, and the contribution of the spin polarization of the core for the $11/2^-$ states of ^{141}Pr, ^{143}Pm, and ^{145}Eu. They were all found to be appreciable in the g-factor calculations. The calculated value are close to the experimental results, but the tendency for the g-factors to vary is not reproduced, as is clear from Fig. 6.

Shell model calculations[7] with a δ-function surface interaction show that the $15/2^+$ wave function is dominated ($\sim 90\%$) by the $[(\pi 1g_{\frac{7}{2}})(\pi 2d_{\frac{15}{2}})^2]^{\frac{15}{2}+}$ configuration. If we use the measured g-factors for single-particle states, $g(\frac{5}{2}^+, {}^{141}\mathrm{Pr}) = 1.654$ and $g(\frac{7}{2}, {}^{141}\mathrm{Pr}) = 0.80\,(3)$ as the effective nucleon g-factors, we find that, for this configuration, $g_{\mathrm{calc}}(15/2^+ = 1.13(3)$, which is in good agreement with experiment. Configurational admixtures, including the $2d_{3/2}$ and $3s_{1/3}$ proton states, have little effect on this result. This is a confirmation of the structure of the $15/2^+$ states and of the theoretical calculations given in Ref. 7.

The relaxation time for the oxide targets is about 25 ns. Interaction with the fluctuating fields due to the paramagnetic ions produces a loss of nuclear orientation. Defects due

TABLE III. Calculated g-factors for the $11/2^-$ states in the quasiparticle phonon model.

Nucleus	C_I^2	g_{sp}	$g_1^{(2)}$	$g_1^{(3)}$	g_2	g_{calc}	g_{meas}
^{141}Pr	0,876	1,417	0,071	0,034	−0,052	1,288	1,13(7)
^{143}Pm	0,894	1,417	0,058	0,023	−0,101	1,238	1,23(8)
^{145}Eu	0,906	1,417	0,049	0,019	−0,127	1,231	1,356(8) *

*Taken from Ref. 13

to radiation damage in the cubic lattice of the target, introduced during annealing and diffusion, produce time-dependent electric-field gradients[29,30] that may give rise to a relaxation of orientation. However, the same relaxation time $\tau_R = 19(6)$ ns has been reported[31] for the $11/2^-$ state of ^{139}Pr in a Ce host at 900 °C. In the cubic lattice of the metal at temperatures $T > 0.6T_{\text{melt}}$, annealing occurs rapidly and the orientation of the nuclei is preserved. This enables us to conclude that the relaxation time observed for the oxide targets was due exclusively to the fields of unfilled 4*f*-shells. The dynamic nature of the interaction producing relaxation is confirmed by the temperature dependence of τ_R (see Table I). According to the theory of Abragam and Pound,[32] the attenuation factor in (1) and (2) is then of the form

$$G_k(t) = \exp(-\lambda_k t). \tag{12}$$

The relaxation time due to the time-dependent interaction is given by[33]

$$1/\tau_R = \lambda_k^{\text{magn}} + \lambda_k^{\text{el}}$$

$$= k(k+1)\{{}^1/_3\omega_M{}^2\tau_c + {}^3/_5[4I(I+1) - k(k+1) - 1]\omega_Q{}^2\tau_c\}, \tag{13}$$

where the magnetic interaction frequency is $\omega_M = -g\mu_N B_i(0)/\hbar$, and the quadrupole interaction frequency is $\omega_Q = e^2Qq/4I(2I-1)\hbar$ (Q is the quadrupole moment and q the electric-field gradient).

The quadrupole moment is of the order of [34] 0.05 barn. If we use $B_i(0)$ and q calculated for the unfilled 4*f*-shells of trivalent ions,[35] the correlation times for the oxide targets turn out to be

$$\tau_c(^{141}\text{Pr}) = 0.5\cdot 10^{-13}\,\text{s}, \quad \tau_c(^{143}\text{Pm}) = 0.8\cdot 10^{-13}\,\text{s}.$$

Such small correlation times are observed only for liquid sources.

The relaxation times are shorter for metal targets. Let us estimate the static quadrupole interaction. The attenuation factor is then[36]

$$G_k(t) = \sum_n s_{kn} \cos n\omega_0 t, \tag{14}$$

where $\omega_0 = 3\omega_Q$ for integral I and $\omega_0 = 6\omega_Q$ for half-integral I. To explain the observed attentuation of $R(\theta, B, t)$, the electricfield gradient must be $\sim 10^{19}$ V/cm. This is greater by a factor of 50 than the result obtained experimentally for Gd in Gd with a similar value of c/a (Ref. 37): $q = 3.4\times 10^{17}$V/cm.

The reduction in the relaxation times obtained for metal targets can be explained on the assumption of: (1) an increased correlation time, or (2) the presence of an additional time-dependent interaction. In the former case, the results for $T \approx 300$ K are

$$\tau_c(^{141}\text{Pr}) = 1.6\cdot 10^{-13}\,\text{s}, \quad \tau_c(^{143}\text{Pm}) = 1.5\cdot 10^{-13}\,\text{s}.$$

For praseodymium in the cerium lattice, $\tau_c = 0.6\times 10^{-13}$ s (Ref. 31) at $T = 1173$ K, i.e., τ_c is very approximately inversely proportional to temperature, which is characteristic for a time-dependent interaction. The second reason for the reduction in τ_R in the case of metal targets can be dynamic interaction during diffusion and the curing of radiation damage present in oxide targets. Detailed measurements of the attenuation factors G_2 and G_4 as functions of time and temperature will be necessary to verify these assumptions.

The authors are grateful to A. V. Kuznichenko, V. N. Lebedev, and G. P. Onishchenko for assistance during the initial stages of this research, and to A. I. Vdovin for useful discussions.

The authors are grateful to A. V. Kuznichenko, V. N. Lebedev, and G. P. Onishchenko for assistance during the initial stages of this research, and to A. I. Vdovin for useful discussions.

[1] B. H. Wildenthal, Phys. Rev. Lett. **22**, 1118 (1969).
[2] K. Heyde and M. Waraquier, Nucl. Phys. A **167**, 545 (1971).
[3] H. Freed and W. Miles, Nucl. Phys. A **158**, 230 (1970).
[4] B. H. Wildenthal, E. Newman, and R. L. Auble, Phys. Rev. C **3**, 1199 (1971).
[5] D. Bazzacco, A. M. I. Haque, K. O. Zell, and P. Brentano, Phys. Rev. C **21**, 222 (1980).
[6] D. A. Rakel, R. Kaczarowski, E. G. Funk, and Z. W. Milelich, Phys. Rev. C **21**, 595 (1980).
[7] H. Prade, L. Käubler, U. Hagemann, *et al.*, Nucl. Phys. A **333**, 33 (1980).
[8] H. Prade, W. Enghardt, H. U. Jäger, *et al.*, Nucl. Phys. A **370**, 47 (1981).
[9] H. Morinaga and T. Yamazaki, In-Beam Gamma-Ray Spectroscopy, North-Holland, Amsterdam, 1976, p 105.
[10] C. Günther and I. Lindgren, Russ. transl. in: Vozmushchennye uglovye korrelyatsii (Perturbed Angular Correlations), Atomizdat, Moscow, 1964, p. 311.
[11] I. I. Zalyubovskiĭ, V. I. Konfederatenko, V. N. Lebedev, and A. I. Levon, Tezisy XXIX Soveshchaniya po yadernoĭ spektroskopii i strukture atomnogo yadra, Riga (Abstracts of the Twenty-Ninth Conf. on Nuclear Spectroscopy and Structure, Riga), 1979, p. 245.
[12] N. D. Kornienko, B. G. Kul'chinskiĭ, A. I. Levon, and O. F. Nemets, Izv. Akad. Nauk SSSR Ser. Fiz. **38**, 156 (1974).
[13] W. Klinger, R. Böhm, W. Engel, *et al.*, Z. Phys. A **290**, 227 (1979); Nucl. Phys. A **350**, 61 (1980).
[14] R. Keiterl, H. H. Bertschat, R. Butt, *et al.*, Z. Phys. A **290**, 229 (1979).
[15] G. Netz, W. Prieske, H. Daum, *et al.*, Hyperfine Interactions **3**, 147 (1977).
[16] A. V. Kusnichenko, V. N. Lebedev, A. I. Levon, and O. F. Nemets, Izv. Akad. Nauk SSSR Ser. Fiz. **41**, 1624 (1977).
[17] M. Darby and K. N. Taylor, Physics of Rare-Earth Solids, Halsted, 1972 (Russian translation, Mir, Moscow, 1974].
[18] L. Käubler, H. Prade, L. Schneider, *et al.*, XV Soveshchanie po yadernoĭ spektroskopii i teorii yadra, Dubna (Fifteenth Conf. on Nuclear Spectroscopy and Nuclear Theory, Dubna), 1978, p. 153.
[19] H. Ejiri, T. Shibata, and M. Takeda, Nucl. Phys. A **221**, 211 (1974).
[20] H. Noya, A. Arima, and H. Horie, Prog. Theor. Phys. Suppl. **8**, 33 (1958).
[21] V. G. Solov'ev, EChAYa **9**, 810 (1978).
[22] V. G. Solov'ev, Teoriya slozhnykh yader (Theory of Complex Nuclei), Nauka, Moscow, 1971.
[23] A. B. Migdal, Zh. Eksp. Teor. Fiz. **19**, 1136 (1963) [sicl]
[24] J. Blomqvist, N. Freed, and H. O. Zetterström, Phys. Lett. **18**, 47 (1965).
[25] J. D. Vergados, Phys. Lett. B **36**, 12 (1971).
[26] A. I. Vdovin, V. V. Voronov, V. Yu. Ponomarev, and I. Stoyanov, Yad. Fiz. **30**, 923 (1979) [Sov. J. Nucl. Phys. **30**, 479 (1979)].
[27] Chan Zuy Khuong, V. G. Soloview, and V. V. Voronov, J. Phys. G. **7**, 151 (1981).
[28] I. Stoyanov and Chan Zuy Khuong, Preprint No. R4-81-234, Dubna, 1981.
[29] H. Bertschat, H. Haas, F. Pleiter, *et al.* Phys. Rev. B **12**, 1 (1975).
[30] R. Butt, H. Haas, T. Butz, *et al.*, Phys. Lett. A **64**, 309 (1977).
[31] T. J. Ketel, E. A. Vervaet, and H. Z. Verheul, A. Phys. Z. **291**, 319 (1979).
[32] A. Abragam and R. N. Pound, Phys. Rev. **92**, 943 (1952).
[33] M. Morinaga and T. Yamazaki, In-Beam Gamma-Ray Spectroscopy, North-Holland, Amsterdam, 1976, p. 424.
[34] C. M. Lederer and V. S. Shirley, Tables of Isotopes, 7th ed., Wiley, New York, 1978.
[35] C. Günther, G. Strube, U. Wehmann, *et al.*, Z. Phys. **183**, 478 (1965).
[36] H. Frauenfelder and R. M. Steffen, in: Alpha-, Beta-, and Gamma-Ray Spectroscopy ed. K. Siegbahn, North-Holand, Amsterdam, 1965 (Russian translation, Atomizdat, Moscow, 1969)
[37] O. Häusser, Hyperfine Interacions **9**, 19 (1983).

Translated by S. Chomet